

# Synthesis of Enantiomers of *exo*-2-Norbornyl-*N*-*n*-butylcarbamate and *endo*-2-Norbornyl-*N*-*n*-butylcarbamate for Stereoselective Inhibition of Acetylcholinesterase

SHYH-YING CHIOU,<sup>1,2</sup> CHUAN-FU HUANG,<sup>1,2</sup> SHYH-JEI YEH,<sup>3</sup> I-RU CHEN,<sup>3</sup> AND GIALIH LIN<sup>3\*</sup>

<sup>1</sup>Department of Neurosurgery, Chung Shan Medical University Hospital, Taichung, Taiwan

<sup>2</sup>School of Medicine, Chung Shan Medical University, Taichung, Taiwan

<sup>3</sup>Department of Chemistry, National Chung-Hsing University, Taichung, Taiwan

**ABSTRACT** The acetylcholinesterase inhibition by enantiomers of *exo*- and *endo*-2-norbornyl-*N*-*n*-butylcarbamates shows high stereoselectivity. For the acetylcholinesterase inhibitions by (*R*)-(+)- and (*S*)-(–)-*exo*-2-norbornyl-*N*-*n*-butylcarbamates, the *R*-enantiomer is more potent than the *S*-enantiomer. But, for the acetylcholinesterase inhibitions by (*R*)-(+)- and (*S*)-(–)-*endo*-2-norbornyl-*N*-*n*-butylcarbamates, the *S*-enantiomer is more potent than the *R*-enantiomer. Optically pure (*R*)-(+)-*exo*-, (*S*)-(–)-*exo*-, (*R*)-(+)-*endo*-, and (*S*)-(–)-*endo*-2-norbornyl-*N*-*n*-butylcarbamates are synthesized from condensations of optically pure (*R*)-(+)-*exo*-, (*S*)-(–)-*exo*-, (*R*)-(+)-*endo*-, and (*S*)-(–)-*endo*-2-norborneols with *n*-butyl isocyanate, respectively. Optically pure norborneols are obtained from kinetic resolutions of their racemic esters by lipase catalysis in organic solvent. *Chirality* 22:267–274, 2010. © 2009 Wiley-Liss, Inc.

**KEY WORDS:** acetylcholinesterase; carbamate inhibitor; enantiomer; stereoselectivity; resolution by lipase

## INTRODUCTION

Acetylcholinesterase (AChE, EC 3.1.1.7) plays a vital role in the central and peripheral nervous systems, where it catalyzes the hydrolysis of the neurotransmitter acetylcholine (ACh).<sup>1</sup> The first X-ray structure of AChE from *Torpedo californica* electric organ has been reported in 1991.<sup>2</sup> Recently, the X-ray structure of AChE with an Alzheimer's disease (AD) drug rivastigmine has also been reported.<sup>3</sup> The active site of AChE consists of at least five major binding sites (see Fig. 1): (a) an oxyanion hole (OAH), Gly118, Gly119, and Ala201, that stabilizes the tetrahedral intermediate; (b) an esteratic site (ES) or catalytic triad Ser200-His440-Glu327; (c) an anionic substrate binding site (AS), Trp84, Glu199, and Phe330, that contains a small number of negative charge but many aromatic residues, where the quaternary ammonium pole of ACh and of various active site ligands binds through a preferential interaction of quaternary nitrogens with the  $\pi$  electrons of aromatic groups; (d) an active site-selective aromatic binding site (AACS) that is contiguous with or near the esteratic and anionic loci and that is important in binding aryl substrates and active site ligands; and (e) an acyl binding site (ABS), Phe288 and Phe299, that binds the acetyl group of ACh.<sup>2–5</sup> Besides five major binding sites, AChE also has a peripheral anionic binding site (PAS), Trp279, Tyr70, Tyr121, Asp72, Glu199, and Phe290 that may bind to 9-aminoacridine, 9-amino-1,2,3,4-tetrahydroacridine (tacrine) and is >20 Å from the active site.<sup>6–9</sup>

In Alzheimer's disease (AD), a neurological disorder, cholinergic deficiency in the brain has been reported.<sup>10,11</sup>

Four drugs for the treatment of AD, tacrine (Cognex), donepezil (Aricept), rivastigmine (Exelon) (see Fig. 2), and galantamine (Reminyl) are inhibitors of AChE.<sup>11–14</sup> The derivatives of physostigmine (see Fig. 2) are also potential drugs for the treatment of AD.<sup>15</sup> Since rivastigmine<sup>16</sup> and physostigmine are carbamates, the inhibition mechanism of AChE by carbamates<sup>17–23</sup> plays important roles for treatment of AD.

Carbaryl (1-naphthyl *N*-methylcarbamate, Sevin) (see Fig. 2), carbofuran (Furadan), propoxur (Baygon), and aldicarb (Temik) are carbamate pesticides that have activities against a broad range of insects and low mammalian toxicity.<sup>24</sup> These carbamate pesticides are potent inhibitors of AChE. Therefore, the inhibition mechanism of AChE by carbamates also plays important roles in understanding the mechanism of pesticide toxicology. Bicyclic monoterpenoids are contained in many kinds of essential oils and are reported as reversible inhibitors of AChE.<sup>25,26</sup> Moreover, AChE does not show significant stereoselectivity for enantiomers of many bicyclic monoterpenoids.

Lipases (EC 3.1.1.3) have been widely used in organic synthesis especially in resolution of many chiral secondary alcohols as the enantiomerically pure starting materials in

Contract grant sponsor: NSC Taiwan

\*Correspondence to: Gialih Lin, Department of Chemistry, National Chung-Hsing University, Taichung 402, Taiwan.

E-mail: gilin@dragon.nchu.edu.tw

Received for publication 21 October 2008; Accepted 16 March 2009

DOI: 10.1002/chir.20739

Published online 3 June 2009 in Wiley InterScience (www.interscience.wiley.com).

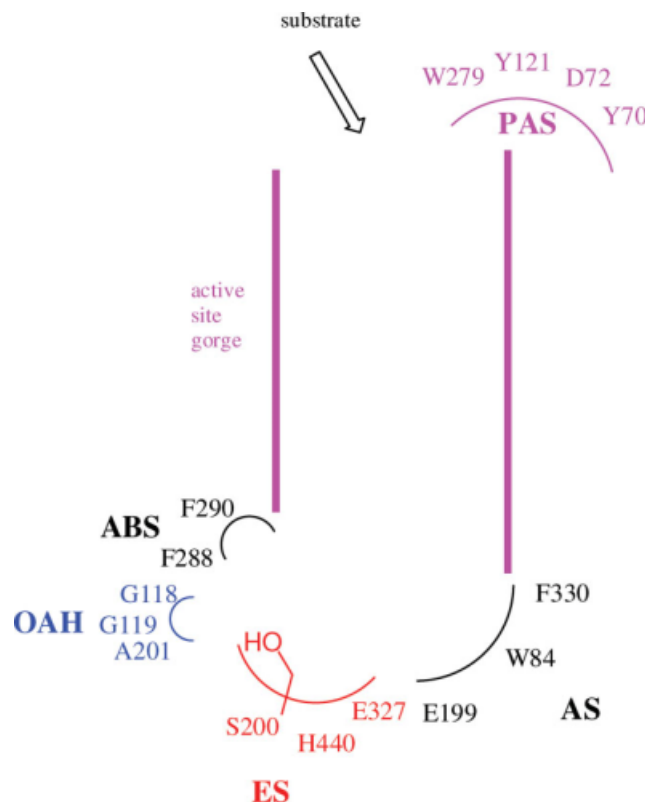


**Fig. 1.** Binding sites of *Torpedo californica* AChE.<sup>2</sup> The enzyme binding sites consist of at least five major binding sites: (a) an oxyanion hole (OAH), (b) an esteratic site (ES) or catalytic triad; (c) an anionic substrate binding site (AS), (d) an acyl binding site (ABS), and (e) a peripheral anionic binding site (PAS). [Color figure can be viewed in the online issue, which is available at [www.interscience.wiley.com](http://www.interscience.wiley.com).]

asymmetric synthesis.<sup>27,28</sup> Therefore, optically pure (*R*)-(+)-*exo*-, (*S*)-(-)-*exo*-, (*R*)-(+)-*endo*-, and (*S*)-(-)-*endo*-2-norborneols are obtained from kinetic resolution of their racemic esters by lipase in organic solvent.

The aim of this work is to study the stereoselectivity for inhibition of AChE by chiral norbornyl-derived carbamates. We have reported that racemic ( $\pm$ )-*exo*- and ( $\pm$ )-*endo*-2-norbornyl-*N*-*n*-butylcarbamates are potent pseudo substrate inhibitors of butyrylcholinesterase (BChE).<sup>29</sup> In this article, we further synthesize optically pure (*R*)-(+)-*exo*-, (*S*)-(-)-*exo*-, (*R*)-(+)-*endo*-, and (*S*)-(-)-*endo*-2-norbornyl-*N*-*n*-butylcarbamates (see Fig. 2) and study the stereoselectivity for inhibition of AChE by these carbamate inhibitors.

## MATERIALS AND METHODS

### Materials

Electric eel AChE (Sigma C2888), porcine pancreatic lipase (Sigma L3126), acetylthiocholine (ATCh), and 5,5'-dithio-bis(-2-nitrobenzoic acid) (DTNB) were obtained from Sigma (USA). ( $\pm$ )-*exo*- and ( $\pm$ )-*endo*-2-Norborneol, *n*-butyl isocyanate, triethylamine, CDCl<sub>3</sub>, tetramethylsilane, *t*-butyl methyl ether, butyryl chloride, pyridine, and (*S*)-(+)- $\alpha$ -methoxy- $\alpha$ -trifluoromethylphenylacetyl chloride

were purchased from Aldrich (USA). Silica gel and TLC plate were obtained from Merck (Germany). Hexane, CH<sub>2</sub>Cl<sub>2</sub>, ethyl acetate, and tetrahydrofuran were obtained from TEDIA (USA). Sodium dihydrogen phosphate (NaH<sub>2</sub>PO<sub>4</sub>·2H<sub>2</sub>O), disodium hydrogen phosphate (Na<sub>2</sub>HPO<sub>4</sub>·12H<sub>2</sub>O), hydrogen chloride (HCl), sodium hydroxide (NaOH), potassium hydroxide (KOH), calcium chloride (CaCl<sub>2</sub>), and sodium chloride (NaCl) were purchased from UCW (Taiwan). Ethanol (95%) was obtained from Taiwan Tobacco & Liquid Corporation (Taiwan).

### Instrumental Methods

All steady-state kinetic data were obtained from an UV-visible spectrophotometer (Agilent 8453) with a cell holder circulated with a water bath. <sup>1</sup>H, <sup>13</sup>C, <sup>19</sup>F NMR spectra were recorded in CDCl<sub>3</sub> at 400, 100, and 377 MHz, respectively, with an internal reference tetramethylsilane (TMS) at 25°C on a Varian Gemini 400 spectrometer. Mass spectra were recorded at 71 eV in a mass spectrometer (Joel JMS-SX/SX 102A). Elemental analyses were performed on a Heraeus instrument. Optical rotation was recorded on a polarimeter (Perkin-Elmer 241).

### Kinetic Resolution of *exo*- and *endo*-2-Norborneols by Lipase (*S*)-(-)-*exo*- and (*R*)-(+)-*exo*-2-Norborneol

To a *t*-butyl methyl ether (100 ml) solution of racemic ( $\pm$ )-*exo*-2-norbornyl butyrate (1 mmol) (synthesis from condensation of ( $\pm$ )-*exo*-2-norborneol with 1.2 equiv of butyryl chloride in the presence of pyridine in CH<sub>2</sub>Cl<sub>2</sub>, 90–95% yield), porcine pancreatic lipase (4 g) was added (Schemes 1 and 2). The reaction mixture was shaken at 36°C at 200 rpm for 72 h. This reaction yielded (*S*)-(-)-*exo*-2-norborneol (49% yield) (mp = 125–126°C and [ $\alpha$ ]<sub>D</sub><sup>25</sup> = -2.70°; [ $\alpha$ ]<sub>D</sub><sup>25</sup> = -3.07° and mp = 126–127°C from literature)<sup>30–34</sup> and recovered unreactive (*R*)-*exo*-2-norbornyl butyrate (51% yield). (*R*)-(+)-*exo*-2-Norborneol (mp = 125–126°C and [ $\alpha$ ]<sub>D</sub><sup>25</sup> = +2.70°) ([ $\alpha$ ]<sub>D</sub><sup>25</sup> = +3.06° and mp = 126–127°C from literature)<sup>30–34</sup> was obtained from basic hydrolysis (0.1 M KOH) of (*R*)-*exo*-norbornyl butyrate in ethanol (95% v/v) in 99% yield.

The enantiomeric excess (ee) values of (*R*)-(+)-*exo*- and (*S*)-(-)-*exo*-2-norborneols from the resolutions were calculated to be 80 and 84%, respectively, from the <sup>19</sup>F NMR spectra of their Mosher's esters as the followings (Fig. 3 and Table 1).<sup>35–37</sup> In a NMR tube, (*R*)-(+)-*exo*-2-norborneol (5 mM) was condensed with the Mosher's chiral derivatizing agent (*S*)-(+)- $\alpha$ -methoxy- $\alpha$ -trifluoromethyl-phenylacetyl chloride<sup>35</sup> (5 mM) in CDCl<sub>3</sub> in the presence of pyridine (5 mM) at 25°C for 24 h (Scheme 3). The fluorine chemical shifts at -73.948 and -74.113 ppm with the integration ratio of 9/1 were assigned to be the fluorine atoms of (2*R*)- and (2*S*)-*exo*-norbornyl-(*S*)- $\alpha$ -methoxy- $\alpha$ -trifluoromethylphenyl acetates, respectively (Scheme 3) (Fig. 3A). Therefore, the enantiomeric excess of (*R*)-(+)-*exo*-2-norborneol from the kinetic resolution by lipase catalysis (Scheme 1) was calculated to be 80% from integration of these two peaks (Table 1).

(*S*)-(-)-*exo*-2-Norborneol (5 mM) was also condensed with the Mosher's chiral derivatizing agent (*S*)-(+)- $\alpha$ -

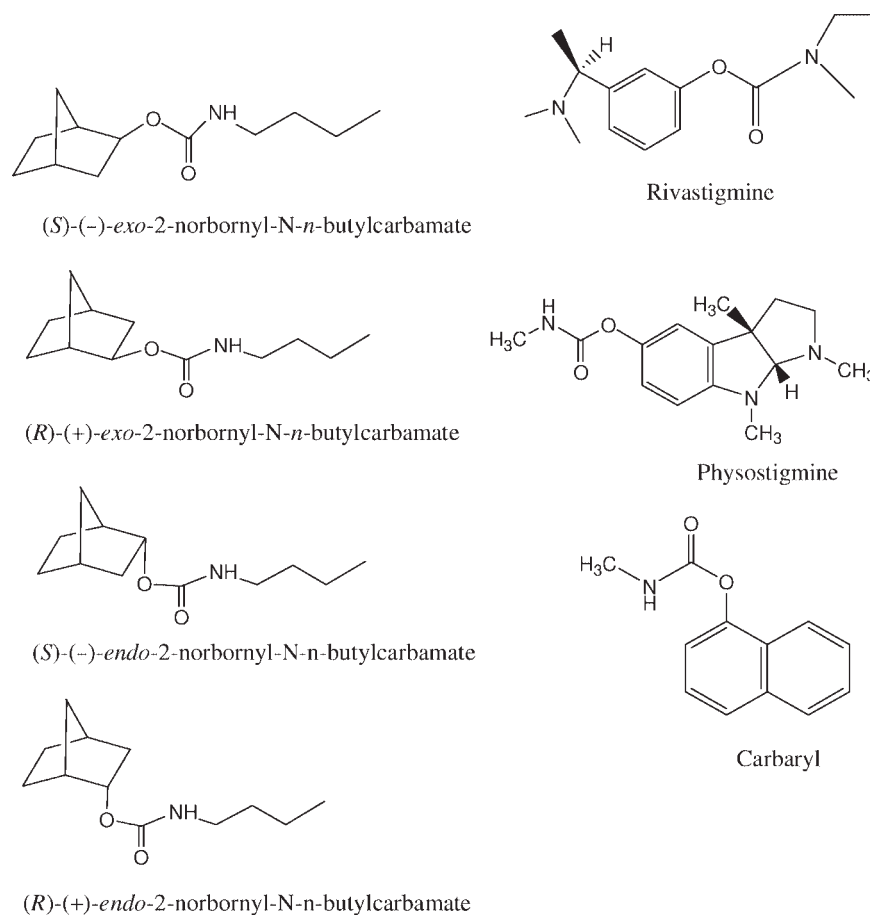
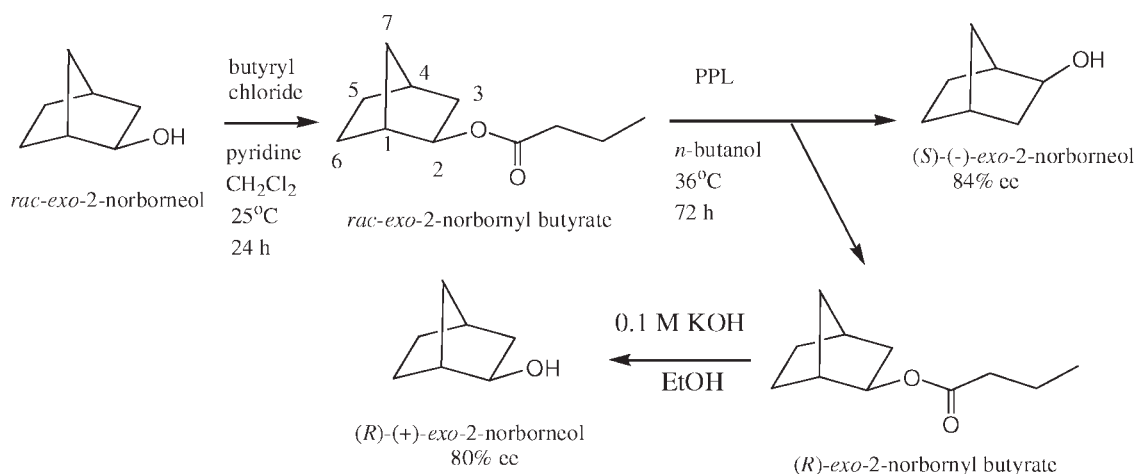


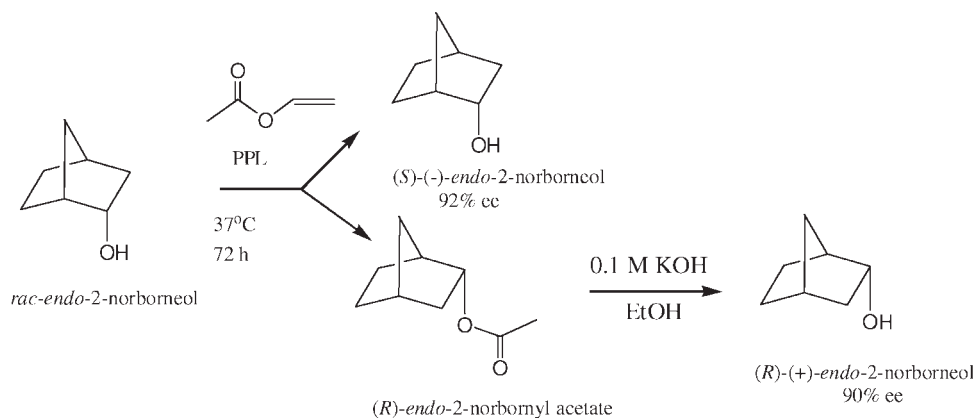
**Fig. 2.** Structures of *(R)*-(+)-*exo*-, *(S)*-(-)-*exo*-, *(R)*-(+)-*endo*-, *(S)*-(-)-*endo*-2-norbornyl-*N*-*n*-butylcarbamates, rivastigmine, physostigmine, and carbaryl.

methoxy- $\alpha$ -trifluoromethylphenyl acetate<sup>35</sup> (5 mM) in  $\text{CDCl}_3$  in the presence of pyridine (5 mM) at 25°C for 24 h (Scheme 3). After reaction, the peaks at -73.965 and -74.130 ppm with the integration ratio of 92/8 were assigned to be the fluorine atoms of (*2R*)- and (*2S*)-*exo*-nor-

bornyl-(*S*)- $\alpha$ -methoxy- $\alpha$ -trifluoromethylphenyl acetates, respectively (Scheme 3 and Fig. 3B). Therefore, the enantiomeric excess of (*R*)-(+)-*exo*-2-norborneol from the kinetic resolution by lipase catalysis was calculated to be 84% (Scheme 1 and Table 1).



**Scheme 1.** Kinetic resolution of (*R*)-(+)- and (*S*)-(-)-*exo*-2-norborneols from lipase-catalyzed hydrolysis of racemic ( $\pm$ )-*exo*-2-norbornyl butyrate.



**Scheme 2.** Kinetic resolution of (*R*)-(+)- and (*S*)-(-)-*endo*-2-norborneols from lipase-catalyzed acetylation of racemic ( $\pm$ )-*exo*-2-norborneol with vinyl acetate.

### (*S*)-(-)-*endo*- and (*R*)-(+)-*endo*-2-Norborneol

To a *t*-butyl methyl ether (50 ml) solution of racemic ( $\pm$ )-*endo*-2-norborneol (44.6 mmol) and vinyl acetate (10 ml), porcine pancreatic lipase (30 g) was added (Scheme 2). The reaction mixture was shaken at 37°C at 200 rpm for 72 h. This reaction yielded (*R*)-(+)-*endo*-2-norbornyl acetate (49%) and recovered unreactive (*S*)-(-)-*endo*-norborneol (51%) (mp = 148–150°C and  $[\alpha]_{\text{D}}^{25} = -1.81^\circ$ ; mp = 151–152°C and  $[\alpha]_{\text{D}}^{25} = -1.89^\circ$  from

literature).<sup>30–34</sup> (*R*)-(+)-*endo*-2-Norborneol (mp = 148–150°C and  $[\alpha]_{\text{D}}^{25} = +1.81$ ;  $[\alpha]_{\text{D}}^{25} = +1.89^\circ$  and mp = 151–152°C from literature)<sup>30–34</sup> was obtained from basic hydrolysis (0.1 M KOH) of (*R*)-*endo*-norbornyl butyrate in ethanol (95%) in 99% yield. The enantiomeric excess (ee) values of (*S*)-(-)-*endo*- and (*R*)-(+)-*endo*-2-norborneols from the resolutions were calculated to be 90 and 92%, respectively, from the <sup>19</sup>F NMR spectra of their Mosher's esters (Table 1).

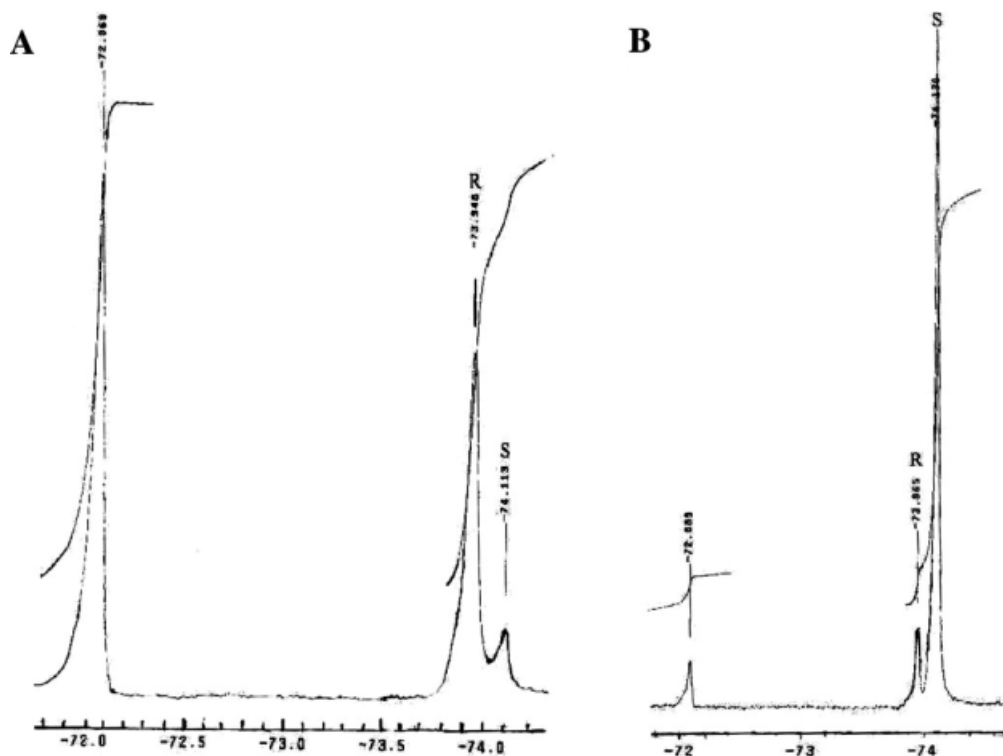


**Fig. 3.** <sup>19</sup>F NMR spectra after the reaction of (A) (*R*)-(-)-*exo*-2-norborneol with *S*-(+)- $\alpha$ -methoxy- $\alpha$ -trifluoromethylphenylacetyl chloride in the presence of pyridine in CDCl<sub>3</sub> and (B) (*S*)-(-)-*exo*-2-norborneol with (*S*)-(+)- $\alpha$ -methoxy- $\alpha$ -trifluoromethylphenylacetyl chloride in the presence of pyridine in CDCl<sub>3</sub>. For (A), -72.069 ppm was the fluorine chemical shift of unreactive (*S*)-(-)- $\alpha$ -methoxy- $\alpha$ -trifluoromethylphenylacetyl chloride. The peaks at -73.948 and -74.113 ppm were assigned to be the fluorine chemical shifts of (*2R*)- and (*2S*)-*exo*-norbornyl-(*S*)- $\alpha$ -methoxy- $\alpha$ -trifluoromethylphenylacetates, respectively (Scheme 3). For (B), -72.089 ppm was the fluorine chemical shift of unreactive (*S*)-(-)- $\alpha$ -methoxy- $\alpha$ -trifluoromethylphenylacetyl chloride. The peaks at -73.965 and -74.130 ppm were assigned to be the fluorine chemical shifts of (*2R*)- and (*2S*)-*exo*-norbornyl-(*S*)- $\alpha$ -methoxy- $\alpha$ -trifluoromethylphenylacetates, respectively (Scheme 3).

**TABLE 1. Enantiomeric excess (%) and optical purity (%) for the kinetic resolution of racemic *exo*-2-norborneol (Scheme 1) and *endo*-2-norborneol (Scheme 2) by lipase in organic solvent**

Compound	Enantiomeric excess (%) <sup>a</sup>	Optical purity (%) <sup>b</sup>
( <i>R</i> )-(+)- <i>exo</i> -2-norborneol	80	88
( <i>S</i> )-(–)- <i>exo</i> -2-norborneol	84	90
( <i>R</i> )-(+)- <i>endo</i> -2-norborneol	90	96
( <i>S</i> )-(–)- <i>endo</i> -2-norborneol	92	96

<sup>a</sup>Enantiomeric excess (%) was calculated from ratio of integration of fluorine chemical shift of their Mosher's ester (Scheme 3) of <sup>19</sup>F NMR spectra (Fig. 3).

<sup>b</sup>Optical purity (%) was calculated as  $100 \times [\alpha]_D^{25} \text{observed} / [\alpha]_D^{25} \text{literature}$ .

In a NMR tube, (*R*)-(+)-*endo*-2-norborneol (5 mM) was condensed with the Mosher's chiral derivatizing agent (*S*)-(+)- $\alpha$ -methoxy- $\alpha$ -trifluoromethylphenylacetyl chloride<sup>35</sup> (5 mM) in CDCl<sub>3</sub> in the presence of pyridine (5 mM) at 25°C for 24 h. The fluorine chemical shifts at –73.975 and –74.152 ppm with the integration ratio of 95/5 were assigned to be the fluorine atoms of (2*R*)- and (2*S*)-*endo*-norbornyl-(*S*)- $\alpha$ -methoxy- $\alpha$ -trifluoromethylphenyl acetates, respectively. Therefore, the enantiomeric excess of (*R*)-(+)-*endo*-2-norborneol from the kinetic resolution by lipase catalysis (Scheme 2) was calculated to be 90% from integration of these two peaks (Table 1).

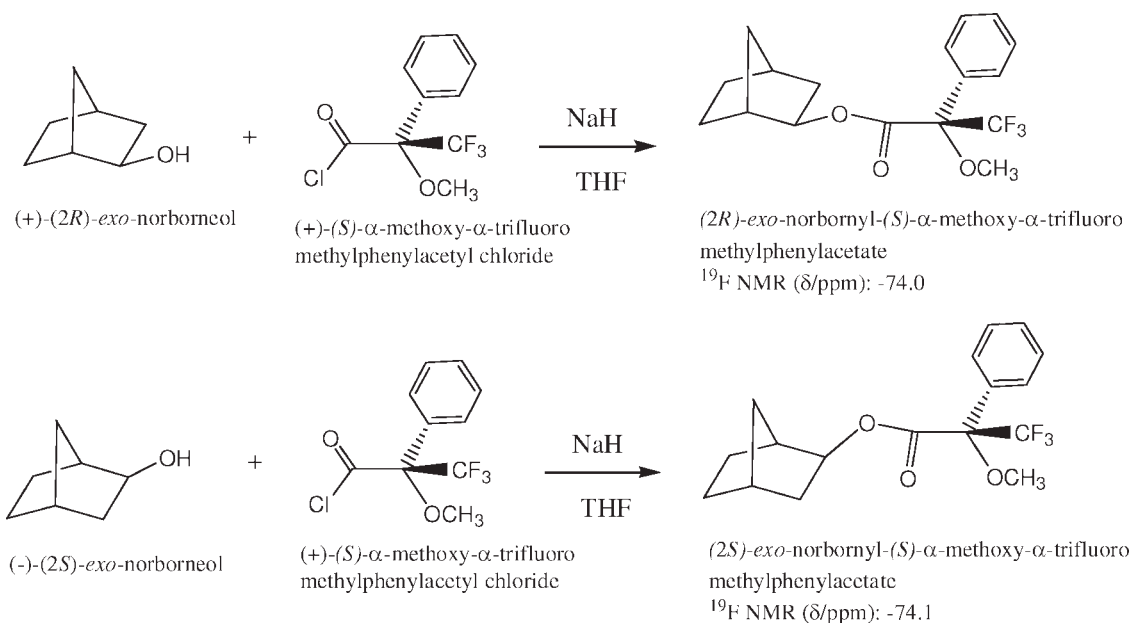
(*S*)-(–)-*endo*-2-Norborneol (5 mM) was condensed with the Mosher's chiral derivatizing agent (*S*)-(+)- $\alpha$ -methoxy- $\alpha$ -trifluoromethylphenylacetyl chloride<sup>35</sup> (5 mM) in CDCl<sub>3</sub> in the presence of pyridine (5 mM) at 25°C for 24 h. The fluorine chemical shifts at –74.026 and –74.185 ppm with the integration ratio of 96/4 were assigned to be the fluorine atoms of (2*R*)- and (2*S*)-*endo*-norbornyl-(*S*)- $\alpha$ -methoxy-

$\alpha$ -trifluoromethylphenyl acetates, respectively. Therefore, the enantiomeric excess of (*S*)-(–)-*endo*-2-norborneol from the kinetic resolution by lipase catalysis (Scheme 2) was calculated to be 92% from integration of these two peaks (Table 1).

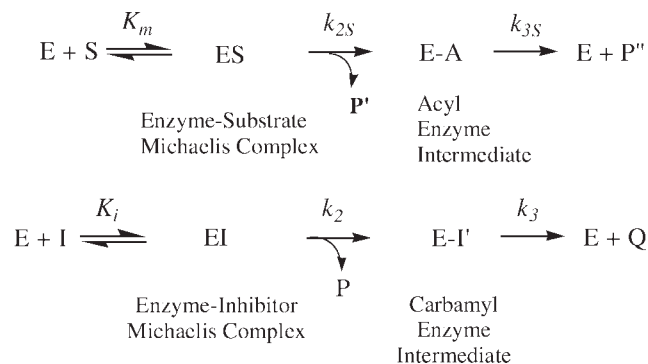
#### Synthesis of (*R*)-(+)-*exo*-, (*S*)-(–)-*exo*-, (*R*)-(+)-*endo*-, and (*S*)-(–)-*endo*-2-Norbornyl-*N*-*n*-butylcarbamates

(*R*)-(+)-*exo*-, (*S*)-(–)-*exo*-, (*R*)-(+)-*endo*-, and (*S*)-(–)-*endo*-2-norbornyl-*N*-*n*-butylcarbamates were synthesized from condensation of optically pure (*R*)-(+)-*exo*-, (*S*)-(–)-*exo*-, (*R*)-(+)-*endo*-, and (*S*)-(–)-*endo*-2-norborneols, respectively, with 1.2 equiv of *n*-butyl isocyanate in the presence of 1.2 equiv of triethylamine in tetrahydrofuran at 25°C for 1 day (85–92% yield). All products were purified by liquid chromatography (silica gel, hexane-ethyl acetate) and were characterized by <sup>1</sup>H and <sup>13</sup>C NMR spectra, mass spectra, and elemental analysis as the followings.

**(*R*)-(+)-*exo*- and (*S*)-(–)-*exo*-2-Norbornyl-*N*-*n*-butylcarbamates.** <sup>1</sup>H NMR (CDCl<sub>3</sub>)  $\delta$  0.92 (t, *J* = 7 Hz, 3H, carbamate  $\omega$ -CH<sub>3</sub>), 1.40 (sextet, *J* = 7 Hz, 2H, carbamate  $\gamma$ -CH<sub>2</sub>), 1.0–1.6 (m, 7H, 4,5,6,7-norbornyl *H*s), 1.56 (quintet, *J* = 7 Hz, 2H, carbamate  $\beta$ -CH<sub>2</sub>), 1.70 (m, 1H, norbornyl C(1)*H*), 2.24 (m, 2H, norbornyl C(3)*H*<sub>2</sub>), 3.15 (t, *J* = 7 Hz, 2H, carbamate  $\alpha$ -CH<sub>2</sub>), 4.53 (m, 1H, norbornyl-C(2)*H*). <sup>13</sup>C NMR (CDCl<sub>3</sub>)  $\delta$  13.7 (carbamate  $\omega$ -CH<sub>3</sub>), 19.9 (carbamate  $\beta$ -CH<sub>2</sub>), 24.2 (norbornyl C-6), 28.1 (norbornyl C-5), 32.1 (carbamate  $\gamma$ -CH<sub>2</sub>), 35.2 (norbornyl C-7), 35.3 (norbornyl C-4), 39.6 (norbornyl C-3), 40.6 (norbornyl C-1), 41.6 (carbamate  $\alpha$ -CH<sub>2</sub>), 77.7 (norbornyl C-2), 156.4 (carbamate C=O). Mass spectra, exact mass: 211.157; elemental analysis: calculated for C<sub>12</sub>H<sub>21</sub>NO<sub>2</sub>: C, 68.21; H, 10.02; N, 6.63, found C, 68.15; H, 10.32; N, 6.56. mp 178–180°C (decomp.).



**Scheme 3.** Determination of enantiomeric excess and absolute configuration of (*R*)-(+)- and (*S*)-(–)-*exo*-2-norborneols by <sup>19</sup>F NMR spectra of their Mosher's ester derivatives.



**Scheme 4.** Kinetic scheme for inhibition of AChE by 2-norbornyl-*N-n*-butylcarbamate in the presence of substrate. E, enzyme; E-A, acyl enzyme; EI, enzyme-inhibitor Michaelis complex; E-I', carbamyl enzyme; ES, enzyme-substrate Michaelis complex; I, pseudo substrate inhibitor;  $k_2$ , carbamylation constant;  $k_3$ , decarbamylation constant;  $k_{2S}$ , formation rate constant of E-A;  $k_{3S}$ , deacylation constant E-A;  $K_i$ , inhibition constant;  $K_m$ , Michaelis-Menten constant; P, product, 2-norborneol; P', product, thiocholine; P'', product, acetate; Q, product, butylcarbamic acid (unstable); S, substrate, ATCh.

**(*R*)-(+)-endo- and (*S*)-(-)-endo-2-Norbornyl-*N-n*-butylcarbamates.**  $^1\text{H}$  NMR ( $\text{CDCl}_3$ )  $\delta$  0.92 (t,  $J = 7$  Hz, 3H, carbamate  $\omega\text{-CH}_3$ ), 1.20–1.80 (m, 11H, carbamate  $\beta$ - and  $\gamma\text{-CH}_2$  and 4,5,6,7-norbornyl *H*s), 1.96 (m, 1H, norbornyl C(1)*H*), 2.10–2.50 (m, 2H, norbornyl C(3)*H*<sub>2</sub>), 3.19 (t,  $J = 7$  Hz, 2H, carbamate  $\alpha\text{-CH}_2$ ), 4.60 (br. s, 1H, carbamate NH), 4.89 (m, 1H, norbornyl-C(2)*H*).  $^{13}\text{C}$  NMR ( $\text{CDCl}_3$ )  $\delta$  13.7 (carbamate  $\omega\text{-CH}_3$ ), 19.8 (carbamate  $\beta\text{-CH}_2$ ), 20.9 (norbornyl C-6), 29.4 (norbornyl C-5), 32.1 (carbamate  $\gamma\text{-CH}_2$ ), 36.4 (norbornyl C-7), 36.9 (norbornyl C-4), 37.2 (norbornyl C-3), 40.4 (carbamate  $\alpha\text{-CH}_2$ ), 40.7 (norbornyl C-1), 75.7 (norbornyl C-2), 156.8 (carbamate C=O). Mass spectra, exact mass: 211.157; elemental analysis: calculated for  $\text{C}_{12}\text{H}_{21}\text{NO}_2$ : C, 68.21; H, 10.02; N, 6.63, found C, 68.17; H, 10.30; N, 6.58. mp 178–180°C (decomp.).

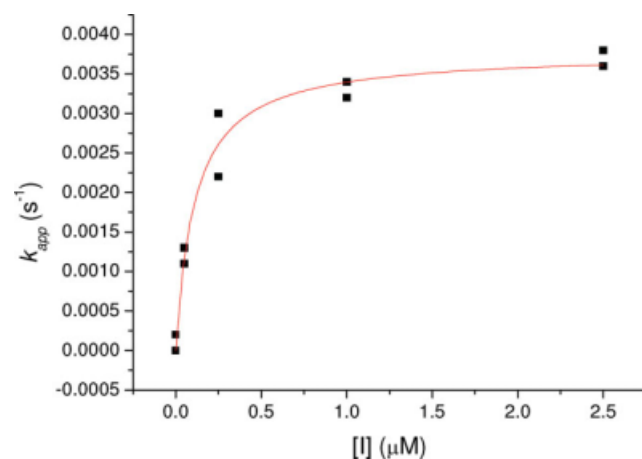


**Fig. 4.** Nonlinear least-squares curve fittings of  $k_{\text{app}}$  vs. (*R*)-(+)-*exo*-2-norbornyl-*N-n*-butylcarbamate concentration ( $[I]$ ) plot following eq 1 for pseudo substrate inhibition of AChE. The parameters of the fit were  $k_2 = 0.0038 \pm 0.0002 \text{ s}^{-1}$  and  $(1 + [S]/K_m) K_i = 110 \pm 20 \text{ nM}$  with  $R = 0.9876$ . After calculation,  $K_i = 56 \pm 10 \text{ nM}$  and  $k_i = (7 \pm 1) \times 10^4 \text{ M}^{-1} \text{ s}^{-1}$  (Table 1). [Color figure can be viewed in the online issue, which is available at [www.interscience.wiley.com](http://www.interscience.wiley.com).]

Chirality DOI 10.1002/chir

**TABLE 2.** The  $k_2$ ,  $K_i$ , and  $k_i$  values<sup>a</sup> of the AChE inhibitions by stereoisomers of 2-norbornyl-*N-n*-butylcarbamates

Inhibitors	$K_i$ (nM)	$k_2$ ( $10^{-3} \text{ s}^{-1}$ )	$k_i$ ( $10^3 \text{ M}^{-1} \text{ s}^{-1}$ ) <sup>b</sup>
( <i>R</i> )-(+)- <i>exo</i> -	$56 \pm 10$	$3.8 \pm 0.4$	$70 \pm 10$
( <i>S</i> )-(-)- <i>exo</i> -	No inhibition <sup>c</sup>	No inhibition <sup>c</sup>	No inhibition <sup>c</sup>
<i>rac</i> -(±)- <i>exo</i> -	$100 \pm 20$	$4.0 \pm 0.3$	$40 \pm 8$
( <i>R</i> )-(+)- <i>endo</i> -	$80 \pm 20$	$8.0 \pm 0.4$	$100 \pm 30$
( <i>S</i> )-(-)- <i>endo</i> -	$20 \pm 5$	$8.0 \pm 0.3$	$400 \pm 50$
<i>rac</i> -(±)- <i>endo</i> -	$50 \pm 10$	$8.2 \pm 0.3$	$160 \pm 30$

<sup>a</sup>The apparent inhibition constant  $(1 + [S]/K_m) K_i$  and carbamylation constant ( $k_2$ ) are obtained from the nonlinear least-squares curve fitting of the  $k_{\text{app}}$  vs.  $[I]$  plot following eq. 1 (Fig. 4).

<sup>b</sup> $k_i = k_2/K_i$ .

<sup>c</sup>No inhibition was observed for the inhibition reaction at the inhibitor concentration of  $10 \mu\text{M}$  for 30 min.

### Data Reduction and Molecular Modeling

Origin (version 6.0) was used for the linear and nonlinear least-squares curve fittings. Molecular structures of (*R*)-(+)- and (*S*)-(-)-*exo*-2-norbornyl-*N-n*-butylcarbamates

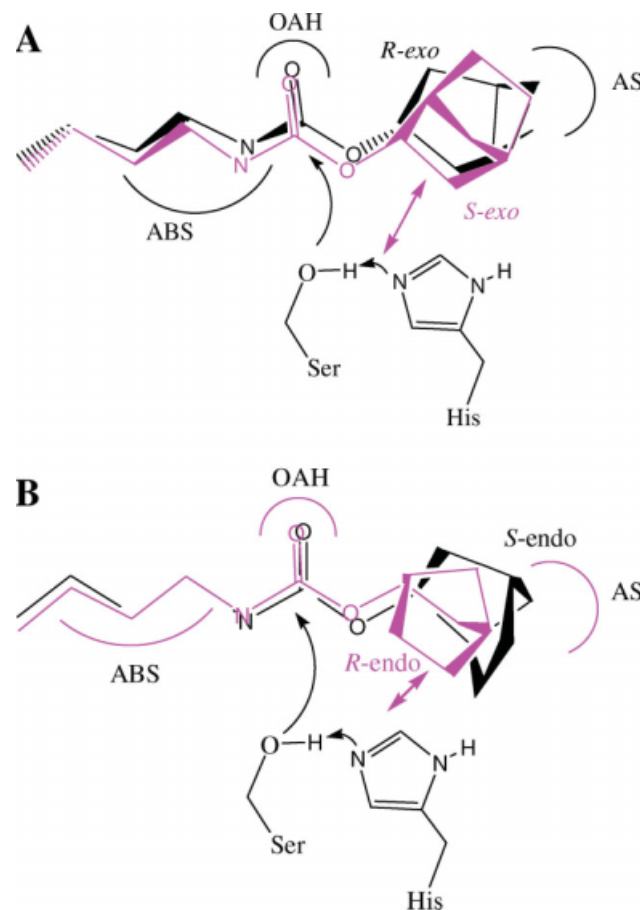


**Fig. 5.** Superimposition of (A) (*R*)-(+)- and (*S*)-(-)-*exo*-2-norbornyl-*N-n*-butylcarbamates and (B) (*R*)-(+)- and (*S*)-(-)-*endo*-2-norbornyl-*N-n*-butylcarbamates at their carbamyl moieties and fitting both enantiomers into the active site of AChE. For (A), unfavorable repulsions between the *S*-enantiomer and the active site serine and histidine of the enzyme were observed. For (B), unfavorable repulsions between the *R*-enantiomer and the active site serine and histidine of the enzyme were observed. [Color figure can be viewed in the online issue, which is available at [www.interscience.wiley.com](http://www.interscience.wiley.com).]

and (*R*)-(+)- and (*S*)-(-)-*endo*-2-norbornyl-*N*-*n*-butylcarbamates shown in Figure were depicted from the molecular structures after MM-2 energy minimization (minimum root mean square gradient was set to be 0.01) by CS Chem 3D (version 6.0).

### Enzyme Inhibition

The AChE inhibition by carbamate inhibitors was assayed by the Ellman method.<sup>38</sup> AChE-catalyzed hydrolysis of ATCh in the presence of carbamate inhibitors and DTNB were followed continuously at 410 nm on a UV-visible spectrometer. The temperature was maintained at 25.0°C by a refrigerated circulating water bath. All inhibition reactions were performed in sodium phosphate buffer (1 ml, 0.1 M, pH 7.0) containing NaCl (0.1 M), acetonitrile (2% by volume), triton X-100 (0.5% by weight), substrate (ATCh) (50 μM), DTNB (50 μM), and varying concentrations of inhibitors ([I] = 0.10, 0.25, 1.0, and 2.5 μM). Requisite volumes of stock solution of substrate and inhibitors in acetonitrile were injected into reaction buffer via a pipette. The inhibition reaction time was 30 min. AChE was dissolved in sodium phosphate buffer (0.1 M, pH 7.0). First-order rate constant ( $k_{app}$ ) for inhibition was determined as described by Hosie et al.<sup>39–41</sup> In the presence of substrate, the kinetic schemes for inhibition of serine hydrolase by carbamate inhibitors had been illustrated (Scheme 4). These reactions were going on simultaneously, with the inhibitor and substrate competing for the active site of the enzyme. In addition, reactivation of the enzyme was insignificant when compared with carbamylation of the enzyme and therefore the  $k_3$  values can be ignored ( $k_2 \gg k_3$ ). Equation 1 was the solution of differential equation that describes the set of reactions depicted in Scheme 4. The apparent inhibition constant ( $1 + [S]/K_m$ )  $K_i$  and carbamylation constant ( $k_2$ ) are obtained from the nonlinear least-squares curve fitting of the  $k_{app}$  vs. [I] plot following eq. 1 (see Fig. 4). The  $K_m$  value for ATCh was obtained as  $50 \pm 10 \mu\text{M}$ . The bimolecular rate constant,  $k_i$ , was defined as  $k_2/K_i$ . Duplicate sets of data were collected for each inhibitor concentration.

$$k_{app} = k_2[I]/(K_i(1 + [S]/K_m) + [I]) \quad (1)$$

## RESULTS AND DISCUSSION

### Kinetic Resolutions of Norborneols by Lipase Catalysis

We first report that optically pure (*R*)-(+)-*exo*-, (*S*)-(-)-*exo*-, (*R*)-(+)-*endo*-, and (*S*)-(-)-*endo*-2-norborneols are kinetically resolved by lipase catalysis in organic solvent (Schemes 1 and 2). The absolute configurations of (*S*)-(-)-*exo*-, (*R*)-(+)-*exo*-, (*S*)-(-)-*endo*-, and (*R*)-(+)-*endo*-2-norborneols are determined on the basis of their optical rotation values<sup>30–34</sup> and the <sup>19</sup>F NMR spectra of their Mosher's esters (Table 1 and Scheme 3).

### 2-Norbornyl-*N*-*n*-butylcarbamates Act as Pseudo Substrate Inhibitors of AChE

The mechanism for AChE-catalyzed hydrolysis of substrate is formation of the first tetrahedral intermediate via nucleophilic attack of the active site serine (see Fig. 1) to

substrate then formation of the acyl enzyme intermediate from the intermediate (Scheme 4). In the presence of substrate, carbamates serve as the pseudo<sup>39–43</sup> or alternate<sup>44,45</sup> substrates inhibitors of AChE. Presumably, the carbamate carbons of the *n*-butylcarbamyl moieties of inhibitors are nucleophilically attacked by the active site serine of the enzyme to form the *n*-butylcarbamyl enzyme (carbamylation).

### Selectivity for the AChE Inhibitions by (*R*)-(+)- and (*S*)-(-)-*exo*-2-Norbornyl-*N*-*n*-butylcarbamates

For the AChE inhibitions by (*R*)-(+)- and (*S*)-(-)-*exo*-2-norbornyl-*N*-*n*-butylcarbamates, *R*-enantiomer is a potent inhibitor but *S*-enantiomer is not an inhibitor (Table 2). Therefore, AChE shows very high stereoselectivity for (*R*)-(+)-*exo*-2-norbornyl-*N*-*n*-butylcarbamates over (*S*)-(-)-*exo*-2-norbornyl-*N*-*n*-butylcarbamate. Modeling both (*R*)-(+)-*exo*- and (*S*)-(-)-*exo*-2-norbornyl-*N*-*n*-butylcarbamates in the active site of AChE<sup>2–5</sup> (see Fig. 1) indicates that the bicyclic norbornyl ring of (*R*)-(+)-*exo*-2-norbornyl-*N*-*n*-butylcarbamate is fitting well into the AS of the enzyme (Fig. 5A). But the bicyclic norbornyl ring of (*S*)-(-)-*exo*-2-norbornyl-*N*-*n*-butylcarbamate is strongly repulsive to the active site serine and histidine (Fig. 5A).

### AChE Inhibitions by (*R*)-(+)- and (*S*)-(-)-*endo*-2-Norbornyl-*N*-*n*-butylcarbamates

For the AChE inhibitions by (*R*)-(+)- and (*S*)-(-)-*endo*-2-norbornyl-*N*-*n*-butylcarbamates, the *S*-enantiomer is four times more potent than the *R*-enantiomer (Table 2). Therefore, AChE shows high stereoselectivity for (*S*)-(-)-*endo*-2-norbornyl-*N*-*n*-butylcarbamates over (*R*)-(+)-*endo*-2-norbornyl-*N*-*n*-butylcarbamate. Modeling both (*R*)-(+)-*endo*- and (*S*)-(-)-*endo*-2-norbornyl-*N*-*n*-butylcarbamates in the active site of X-ray structure of AChE (see Fig. 1)<sup>2–5</sup> indicates that the bicyclic norbornyl ring of (*S*)-(-)-*endo*-2-norbornyl-*N*-*n*-butylcarbamate is fitting well into the AS of the enzyme (Fig. 5B). On the other hand, the bicyclic norbornyl ring of (*R*)-(+)-*endo*-2-norbornyl-*N*-*n*-butylcarbamate is repulsive to the active site serine and histidine (Fig. 5B).

In conclusion, the stereoselectivity of AChE with respect to norbornyl-derived carbamates can be demonstrated for the first time. Among the four stereoisomers of the 2-norbornyl-*N*-*n*-butylcarbamates, (*S*)-(-)-*endo*-stereoisomer is the best inhibitor. It can therefore be concluded that unfavorable repulsions diminish the affinity when the *endo*-substituted inhibitor is (*R*)-configured at the norbornyl moiety. For the *exo*-derivatives, an opposite conclusion can be drawn.

## LITERATURE CITED

1. Quinn DM. Acetylcholinesterase: enzyme structure, reaction dynamics, and virtual transition states. *Chem Rev* 1987;87:955–979.
2. Sussman JL, Harel M, Frolow F, Oefner C, Goldman A, Toker L, Silman I. Atomic structure of acetylcholinesterase from *Torpedo californica*: a prototypic acetylcholine-binding protein. *Science* 1991; 253: 872–879.
3. Harel M, Sussman JL, Krejci E, Bon S, Chanal P, Massoulie J, Silman I. Quaternary ligand binding to aromatic residues in the active-site gorge of acetylcholinesterase. *Proc Natl Acad Sci USA* 1992;89:10827–10831.

4. Bar-On P, Millard CB, Harel M, Dvir H, Enz A, Sussman JL, Silman I. Kinetic and structural studies on the interaction of cholinesterase with anti-Alzheimer drug rivastigmine. *Biochemistry* 2002;41:3555.
5. Harel M, Quinn DM, Nair HK, Silman I, Sussman JL. The X-ray structure of a transition state analog complex reveals the molecular origins of the catalytic power and substrate specificity of acetylcholinesterase. *J Am Chem Soc* 1996;118:2340–2346.
6. Radic Z, Pickering NA, Vellom DC, Camp S, Taylor P. Three distinct domains in the cholinesterase molecule confer selectivity for acetyl- and butyrylcholinesterase inhibitors. *Biochemistry* 1993;32:12074–12084.
7. Taylor P, Mayer RT, Himel CM. Conformers of acetylcholinesterase: a mechanism of allosteric control. *Mol Pharmacol* 1994;45:74–83.
8. Pang Y-P, Quiram P, Jelacic T, Hong F, Brimjoin S. Highly potent, selective, and low cost bis-tetrahydroaminacrine inhibitors of acetylcholinesterase. Steps toward novel drugs for treating Alzheimer's disease. *J Biol Chem* 1996;271:23646–23649.
9. Lin G, Tsai HJ, Tsai YH. Cage amines as the stopper inhibitors of cholinesterases. *Bioorg Med Chem Lett* 2003;13:2887–2890.
10. Mesulam M. Neuroanatomy of cholinesterase in the normal human brain and in Alzheimer's disease. In: Giacobini E, editor. *Cholinesterase and cholinesterase inhibitors*. London: Martin Donitz; 2000. p 121–137.
11. Giacobini E. Cholinergic functions in Alzheimer's disease. *Int J Geriatr Psychiatry* 2003;18:S1–S5.
12. Greig NH, Utsuki T, Yu Q-S, Zhu X, Holloway HW, Perry T, Lee B, Ingram DK, Lahiri DK. A new therapeutic target in Alzheimer's disease treatment: attention to butyrylcholinesterase. *Curr Med Res Opin* 2001;17:1–6.
13. Mesulam MM, Guillozet A, Shaw P, Levey A, Duysen EG, Lockridge O. Acetylcholinesterase knockouts establish central cholinergic pathways and can use butyrylcholinesterase to hydrolyze acetylcholine. *Neuroscience* 2002;110:627–639.
14. Giacobini E, Spiegel R, Enz A, Veroff AE, Cutler NR. Inhibition of acetyl- and butyrylcholinesterase in the cerebrospinal fluid of patients with Alzheimer's disease by rivastigmine: correlation with cognitive benefit. *J Neural Transm* 2002;109:1053–1065.
15. Yu Q-S, Holloway HW, Flippen-Anderson JL, Hoffman B, Brossi A, Greig NH. Methyl analogues of the experimental Alzheimer's drug pheneserine: synthesis and structure/activity relationships for acetyl- and butyrylcholinesterase inhibitory action. *J Med Chem* 2001;44:4062–4071.
16. Bartolucci C, Perola E, Cellai L, Brufani M, Lamba D. Back door opening implied by the crystal structure of a carbamoylated acetylcholinesterase. *Biochemistry* 1999;38:5714–5719.
17. Lin G, Lai C-Y, Liao W-C. Molecular recognition by acetylcholinesterase at the peripheral anionic site: structure-activity relationships for inhibitions by aryl carbamates. *Bioorg Med Chem* 1999;7:2683–2689.
18. Lin G, Lai C-Y, Liao W-C, Liao P-S, Chan C-H. Structure-activity relationships as probes to the inhibition mechanisms of acetylcholinesterase by aryl carbamates. I. The steady-state kinetics. *J Chin Chem Soc* 2003;50:1259–1265.
19. Lin G. Structure-activity relationships as probes to the inhibition mechanisms of acetylcholinesterase by aryl carbamates. II. Hammett-Taft cross-interaction correlations. *J Chin Chem Soc* 2004;51:432–429.
20. Lin G, Liu Y-C, Lin Y-F, Wu Y-G. Ortho effects in quantitative structure-activity relationships for acetylcholinesterase inhibition by aryl carbamates. *J Enzyme Inhib Med Chem* 2004;19:395–401.
21. Lin G, Liao W-C, Chan C-H, Wu Y-H, Tsai H-J, Hsieh C-W. Quantitative structure-activity relationships for the pre-steady state acetylcholinesterase inhibition by carbamates. *J Biochem Mol Toxicol* 2004;18:353–360.
22. Lin G, Tseng H-C, Chio A-C, Tseng T-M, Tsai B-Y. A rate determining step change in the pre-steady state of acetylcholinesterase inhibitions by 1,*n*-alkane-di-*N*-butylcarbamates. *Bioorg Med Chem Lett* 2005;15:951–955.
23. Lin G, Lee Y-R, Liu Y-C, Wu Y-G. Ortho effects for inhibition mechanisms of butyrylcholinesterase by *O*-substituted phenyl *N*-butyl carbamates and comparison with acetylcholinesterase, cholesterol esterase, and lipase. *Chem Res Toxicol* 2005;18:1124–1131.
24. Baron RL. Carbamate insecticides. In: Hayes WJJ, Laws ERJ, editors. *Handbook of pesticide toxicology*, Vol.3. New York: Academic Press; 1991.
25. Miyazawa M, Watanabe H, Umemoto K, Kameoka H. Inhibition of acetylcholinesterase activity by essential oil of *Mentha* species. *J Agric Food Chem* 1998;46:3431–3434.
26. Miyazawa M, Yamafuji C. Inhibition of acetylcholinesterase activity by bicyclic monoterpenoids. *J Agric Food Chem* 2005;53:1765–1768.
27. Boland W, Frössl C, Lorenz N. Esterolytic and lipolytic enzymes in organic synthesis. *Synthesis* 1991;12:1049–1072.
28. Theil F. Lipase-supported synthesis of biologically active compounds. *Chem Rev* 1995;95:2203–2227.
29. Lin G, Chen G-H, Ho H-C. Conformationally restricted carbamate inhibitors of horse serum butyrylcholinesterase. *Bioorg Med Chem Lett* 1998;8:2747–2750.
30. Irwin AJ, Jones JB. Stereoselective horse liver alcohol dehydrogenase catalyzed oxidoreductions of some bicyclic [2.2.1] and [3.2.1] ketones and alcohols. *J Am Chem Soc* 1976;98:8476–8482.
31. Berson JA, Walla JS, Remanick A, Suzuki S, Reynods-Warnhoff P, Willner D. The absolute configurations of some simple norbornane derivatives. A test of the "conformational asymmetry" model. *J Am Chem Soc* 1961;83:3986–3997.
32. Nakazaki M, Chikamatsu H, Naemura K, Asao M. Microbial stereodifferentiating reduction of carbonyl compounds: proposed quadrant rule. *J Org Chem* 1980;45:4432–4440.
33. Winstein S, Trifan D. Neighboring carbon and hydrogen. XI. Solvolysis of exo-norbornyl *p*-bromobenzenesulfonate. *J Am Chem Soc* 1951;74:1154–1160.
34. Yoshizako F, Nishimura A, Chubachi M, Kirihata M. Microbial reduction of 2-norbornanone by *Chlorella*. *J Ferment Bioeng* 1996;82:601–603.
35. Dale JA, Mosher HS. Nuclear magnetic resonance enantiomer reagents. Configurational correlations via nuclear magnetic resonance chemical shifts of diastereomeric mandelate, *O*-methylmandelate, and  $\alpha$ -methoxy- $\alpha$ -trifluoromethylphenylacetate (MTPA) esters. *J Am Chem Soc* 1973;95:512–519.
36. Takahashi T, Fukuishima A, Tanaka Y, Takeuchi Y, Kabuto K, Kabuto C. CFTA, a new efficient agent for determination of absolute configurations of chiral secondary alcohols. *Chem Commun* 2000:788–789.
37. Takahashi T, Kameda H, Kamei T, Ishizaki M. Synthesis of 1-fluoroindan-1-carboxylic acid (FICA) and its properties as a chiral derivatizing agent. *J Fluor Chem* 2006;127:760–768.
38. Ellman CL, Courtney KD, Andres VJ, Featherstone RM. A new rapid colorimetric determination of acetylcholinesterase activity. *Biochem Pharm* 1961;7:88–95.
39. Hosie L, Sutton LD, Quinn DM. *p*-Nitrophenyl and cholesteryl-*N*-alkyl carbamates as inhibitors of cholesterol esterase. *J Biol Chem* 1987;262:260–264.
40. Feaster SR, Lee K, Baker N, Hui DY, Quinn DM. Molecular recognition by cholesterol esterase of active site ligands: structure-reactivity effects for inhibition by aryl carbamates and subsequent carbamyl-enzyme turnover. *Biochemistry* 1996;35:16723–16734.
41. Feaster SR, Quinn DM. Mechanism-based inhibitors of mammalian cholesterol esterase. *Methods Enzymol* 1997;286:231–252.
42. Lin G, Lai C-Y. Hammett analysis of the inhibition of pancreatic cholinesterase by substituted phenyl-*N*-butylcarbamate. *Tetrahedron Lett* 1995;36:6117–6120.
43. Lin G, Shieh C-T, Ho H-C, Chouhwang J-Y, Lin W-Y, Lu C-P. Structure-reactivity relationships for the inhibition mechanism at the second alkyl-chain-binding site of cholesterol esterase and lipase. *Biochemistry* 1999;38:9971–9981.
44. Pietsch M, Gütschow M. Alternate substrate inhibition of cholesterol esterase by thieno[2,3-*d*][1,3]oxazin-4-ones. *J Biol Chem* 2002;277:24006–24013.
45. Pietsch M, Gütschow M. Synthesis of tricyclic 1,3-oxazin-4-ones and kinetic analysis of cholesterol esterase and acetylcholinesterase inhibition. *J Med Chem* 2005;48:8270–8288.